A Comparison on Finite-Set Model Predictive Torque Control Schemes for PMSMs

Omar Sandre-Hernandez, Jose Rangel-Magdaleno, *Senior Member, IEEE*, and Roberto Morales-Caporal, *Senior Member, IEEE*

***Abstract*—This paper introduces the comparison of four predictive torque control schemes for a permanent-magnet synchronous machine (PMSM). The first method is the finite-set model predictive control (FS-MPC). In FS-MPC, the optimal switching state is selected based on the evaluation and minimization of a cost function for all possible voltage space vectors (VSVs) of the inverter. The second method performs a simplified FS-MPC where the selection and evaluation of the possible VSVs are reduced to only three. The third method is based on the principle of predictive direct torque control (PDTC), where the duty cycle of the switching state is optimized for application in the inverter. Finally, a method that combines FS-MPC and PDTC named model predictive torque control is presented. This paper introduces the methodology and the results of a comprehensive comparison of the four predictive schemes based on different criterions. The control schemes are implemented on a field-programmable gate array and are applied to a PMSM. Experimental results are presented to validate the presented comparison and discussion.**

***Index Terms*—Field-programmable gate array, permanent-magnet synchronous machine (PMSM), predictive control, torque control.**

ACRONYMS

AVSV	Active voltage space vector.
CCS-MPC	Continues-control-set model predictive control.
DTC	Direct torque control.
FCS-MPC	Finite-control-set model predictive control.
FOC	Field-oriented control.
FS-MPC	Finite-set model predictive control.
GPC	Generalized predictive control.
MPC	Model predictive control.
MPTC	Model predictive torque control.
PDTC	Predictive direct torque control.
PMSM	Permanent-magnet synchronous machine.
SFS-MPC	Simplified finite-set model predictive control.
VSI	Voltage source inverter.
VSV	Voltage space vector.
ZVSV	Zero-voltage space vector.

Manuscript received June 22, 2017; revised August 11, 2017; accepted November 20, 2017. Date of publication November 27, 2017; date of current version July 15, 2018. The work of O. Sandre-Hernandez was supported by the doctoral scholarship (No. 250561) given by the National Council of Science and Technology (CONACYT), México. Recommended for publication by Associate Editor Dr. B. Fahimi. *(Corresponding author: Omar Sandre-Hernandez.)*

O. Sandre-Hernandez and J. Rangel-Magdaleno are with the Department of Electronics, National Institute for Astrophysics, Optics and Electronics, Puebla 72840, México (e-mail: omarsan@inaoep.mx; jrangel@inaoep.mx).

R. Morales-Caporal is with the Postgraduate Studies and Research Division, Technological Institute of Apizaco, Tlaxcala 90300, México (e-mail: rmcaporal@ieee.org).

Color versions of one or more of the figures in this paper are available online at http://ieeexplore.ieee.org.

Digital Object Identifier 10.1109/TPEL.2017.2777973

I. INTRODUCTION

TODAY, field-oriented control (FOC) and direct torque control (DTC) are two well-established control schemes for electrical drives [1]; however, in recent years, model predictive control (MPC) schemes have received wide attention due to their high performance, natural digital implementation, multivariable control, and inclusion of constraints and nonlinearities in the control objectives [2]. The objective of MPC in electrical drives is to optimize the switching state that will be applied to the voltage source inverter (VSI) based on the model of the machine, this is possible because of the existence of accurate linear mathematical models, which are used to predict the behavior of the controlled variables (typically one step ahead in time) in order to select the final switching state, in this manner, the control becomes an optimization problem solved in real time. MPC entails a wide variety of control techniques, and have been classified into two main categories: continues control set MPC (CCS-MPC) and finite control set MPC (FCS-MPC) [3]. In the first type, an open-loop receding horizon optimization problem is solved during each sampling time, and the control action is applied through a modulator, this is the case of generalized predictive control (GPC) [4], [5]. On the other hand, FCS-MPC exploits the inherent discrete nature of the power converter to solve the optimization problem. FCS-MPC schemes for electrical machines include: finite-set model predictive control (FS-MPC) [6]–[20] and predictive direct torque control (PDTC) [21]–[24].

FS-MPC is one of the more popular predictive control schemes and has been applied in the current [10]–[12], torque [13]–[15], and speed control of electrical machines [16], [17]. In FS-MPC, the discrete behavior of the VSI is used to perform the control; due to the limited number of possible switching states, it is possible to predict the effect of each voltage space vector (VSV) to determine the best VSV for the next sampling time. This process is executed by using a cost function, which defines the control objectives, and the VSV that minimizes the error on the controlled variables is selected for application in the VSI. It is evident that FS-MPC is more efficient than the conventional DTC because the heuristic switching table is replaced

by an optimization procedure; however, the main drawback of this control technique is the high computational burden, especially when the horizon of prediction is bigger than one. For this reason, improving the performance and reducing the complexity of the FS-MPC has recently become an important research topic. Nowadays, several methods to reduce the complexity and the number of calculations in the FS-MPC have been presented in the literature, for instance: sphere decode algorithm [18], the nearest two adjacent vectors [19], single prediction method [20], and branch and bound algorithms [21]. From this methods, [18] and [21] present a complex solution to reduce the computational burden of FS-MPC, while [20] cannot be easily extrapolated to electrical machines, however, the proposed method in [19] is a suitable solution for the control of electrical machines. In this paper, the simplified FS-MPC (SFS-MPC) [19], which uses active prediction vectors, is investigated for comparison in a permanent-magnet synchronous machine (PMSM).

On the other hand, it is well known that the application of one voltage vector during the whole control cycle leads to a high ripple in the controlled variables, for this reason, the sampling frequency of FS-MPC has to be high [27], which requires a fast digital platform in order to reach the computational time. An alternative to overcome this problem is to use a different control technique such as the PDTC. In PDTC rather than applying the switching state during the whole sampling time, two voltage vectors of the VSI are applied to the machine during each sampling time: one active voltage space vector (AVSV) and one zero-voltage space vector (ZVSV), this permits the use of a bigger sampling time with the advantage of a fixed switching frequency. PDTC uses a modulator to apply the AVSV and the ZVSV during their corresponding times, however, it still can be considered as a FCS-MPC scheme because the selection of the optimal VSV is based on the direct evaluation of the effects of discrete states of the power converter in the flux and torque of the PMSM. In PDTC, the duty-cycle optimization can be performed to reach different control objectives, in [25], three different methods are presented to determine the optimal duty cycle for DTC, which includes the deadbeat control, direct mean torque control, and the reduction of the torque ripple root mean square (RMS) value. These methods are highly dependent on the machine parameters, which can be a problem when the parameters vary during operation, for this reason, in [26], a simplification of the duty-cycle calculation is introduced to replace the torque derivatives with weighting factors, however, these factors are calculated trough trial-and-error, which it is not a simple task. In PDTC, the criterion to select the optimal switching state of the VSI is usually based on a second flux prediction [22], [23], this is commonly seen as a drawback of the PDTC because of the math simplifications used to determine it. In order to improve the switching state selection, a control scheme that combine some characteristics of the FS-MPC and PDTC have been presented, this predictive control is called model predictive torque control (MPTC) [27]–[29]. In MPTC, every switching state is evaluated according to the FS-MPC, in this way, flux and torque evaluation is ensured in the vector selection and the one minimizing the cost function is selected for the duty-cycle optimization based on the methods introduced in [25] and [26]. The introduction of different control schemes has led to a large number of possibilities to perform an optimal control of electrical machines, including the classic control schemes like FOC and DTC, and the different predictive control schemes; however, in terms of optimal torque performance, it is difficult to give an exact idea of which one gives the best results mainly because these controllers are commonly implemented on different machines with different parameters.

From the several predictive schemes in the literature, two principles of operation are the most popular: those that optimize the switching state for application during the whole control cycle (FS-MPC and SFS-MPC); and those which optimize the duty cycle of the switching state (PDTC and MPTC). Although from the theoretical point of view FS-MPC, SFS-MPC, and the MPTC present a significant similitude on the principle used to optimize the switching state, in real experimental evaluation these control schemes might result in a varied steady-state performance of torque, stator flux, and current ripple [13]. So far, some papers have addressed the comparison between predictive schemes [6], [10]–[14], [27], and [28]; however, in these comparisons, the classic vector control and the predictive control schemes are compared [6], [11], [13], hence, is evident that the performance of the digital implementation of predictive schemes is superior than classic schemes. Other papers have addressed the comparison performed on the same predictive control scheme but pursuing different control objectives, for example, in [10] and [12], a comparison between torque and current control for the FS-MPC is presented; in [14], a comparison between flux and torque control is introduced; and in [27] and [28], the evaluation of MPTC with different duty-cycle optimizations is presented. Yet, a comparison on more complex predictive schemes have not been presented, moreover, predictive schemes with different principles of operation like the FS-MPC, SFS-MPC, PDTC, and the MPTC have only been compared when they were first introduced, however, a comparison of these schemes is not possible because they were carried out under different machines and it is not a simple task to conclude which one is the more suitable for certain applications. For this reason, the main contribution of this paper is the comparison and evaluation of some of the most common predictive schemes that aims to optimize the torque performance of a PMSM. Two principles of operation are compared: the optimization of the switching state based on a cost function (FS-MPC and SFS-MPC), and the optimization based on duty-cycle optimization (PDTC and MPTC). FS-MPC and PDTC are selected as these schemes represent the most used predictive controls in the literature and are the basic schemes for more complex strategies; however, in contrast with PDTC, where only three VSVs are evaluated during each control cycle, in FS-MPC, a full evaluation of the VSVs of the VSI is carried out, for this reason, to accomplish a fair comparison, SFS-MPC is selected, here, only three VSVs are selected for evaluation during each control cycle. Finally, MPTC is presented to compare the case when full evaluation of the VSVs with duty-cycle optimization is done. These strategies are evaluated experimentally using various criteria to give an objective evaluation. The results provide a guide for users to obtain an idea of which control scheme should be selected to accomplish their control objectives.

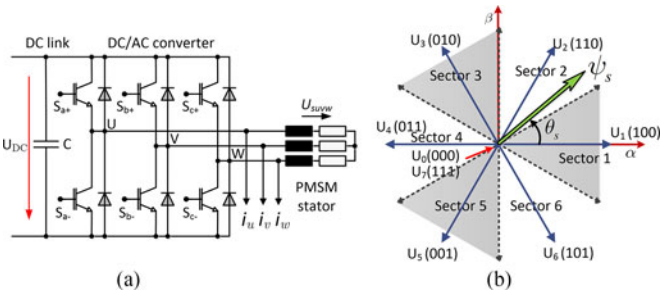

Fig. 1. Two-level voltage source inverter. (a) Topology of the power converter connected to the stator of the PMSM. (b) Output voltages generated by the switching states in the α–β plane.

II. Discrete Model of the PMSM

In order to provide the voltage to the PMSM a two-level VSI is used and is shown in Fig. 1(a). With this topology, eight different combinations are obtained through the gate signals S_x, six AVSVs and two ZVSVs, and can be represented in the complex plane α–β as shown in Fig. 1(b).

The voltage equation of the PMSM in continuous time can be expressed in the stator reference frame (α–β) as in [23]; however, predictive control schemes are carried out with a discrete-time model of the machine, therefore, a discretization of the mathematical model of the PMSM is performed based on the Euler forward differentiation method for the discrete time $(k+1)$ as

$$i_\alpha(k+1) = i_\alpha(k) + \frac{Ts}{L}\left(u_\alpha(k) - R\cdot i_\alpha(k) + \cdots w_r \cdot \psi_{\mathrm{PM}} \cdot \sin\gamma_e(k)\right) \tag{1a}$$

$$i_\beta(k+1) = i_\beta(k) + \frac{Ts}{L}\left(u_\beta(k) - R\cdot i_\beta(k) - \cdots w_r \cdot \psi_{\mathrm{PM}} \cdot \cos\gamma_e(k)\right) \tag{1b}$$

$$\psi_{\alpha,\beta}(k+1) = \psi_{\alpha,\beta}(k) + Ts\left(u_{\alpha,\beta}(k) - R\cdot i_{\alpha,\beta}(k)\right) \tag{2}$$

$$M_e(k+1) = \frac{3}{2}p\cdot\left(\psi_\alpha(k+1)\cdot i_\beta(k+1) - \psi_\beta(k+1)\cdot i_\alpha(k+1)\right) \tag{3}$$

$$\gamma_e(k+1) = \gamma_e(k) + Ts\cdot w_r \tag{4}$$

where $u_{\alpha,\beta}$, $\psi_{\alpha,\beta}$, and $i_{\alpha,\beta}$ are the α–β orthogonal components of voltage, flux, and current space vector, respectively, R is the stator resistance, L is the stator inductance, ψ_{PM} is the PM excited flux, w_r is the electrical speed, M_e is the electromagnetic torque, p is the number of pole pairs, γ_e and γ_m are the electrical and mechanical angular position of the rotor, respectively, and Ts is the sampling time.

III. Control Strategies

In this section, the predictive control strategies are presented. They are divided according to their control principle into the strategies that optimize the switching state applied during the full control cycle (FS-MPC and SFS-MPC), and the ones that optimize the switching state introducing a duty-cycle optimization (PDTC and MPTC). Since FS-MPC, SFS-MPC, and MPTC present a similar control law, they have been represented using a simplified block diagram shown in Fig. 2. FS-MPC blocks are within the black dashed line; SFS-MPC blocks are within the black and red dashed lines; and MPTC blocks are within the black and blue dashed lines.

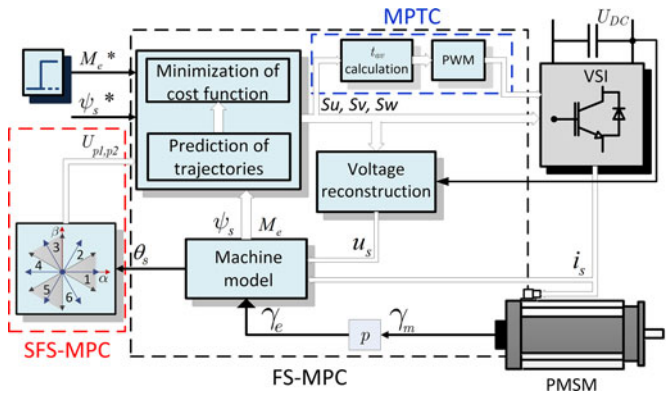

Fig. 2. Simplified block diagram of FS-MPC (black dashed line), SFS-MPC (black plus red dashed lines), and MPTC (black plus blue dashed lines).

TABLE I
Voltage Reconstruction

Switching State	U_0 000	U_1 100	U_2 110	U_3 010	U_4 011	U_6 101	U_7 111
$\upsilon_\alpha/U_{\mathrm{DC}}$	0	2/3	1/3	−1/3	−2/3	1/3	0
$\upsilon_\beta/U_{\mathrm{DC}}$	0	0	$1/\sqrt{3}$	$1/\sqrt{3}$	0	$-1/\sqrt{3}$	0

A. FS-MPC and SFS-MPC

A simplified block diagram of the FS-MPC is shown in Fig. 2. It comprises three blocks: the voltage reconstruction, the estimation of the machine variables, and the predictive control. At each sampling instant, the stator currents, the mechanical angular position of the rotor, and the voltage in the dc link are measured, after this, the voltage applied to the machine is calculated based on Table I, then, the stator flux and torque of the machine are estimated using the dynamic model, and finally, the predictive control is carried out.

FS-MPC is divided into two tasks: the prediction of the controlled variables and the evaluation and minimization of the cost function. In the first one, the prediction of the stator flux and torque based on the discrete model of the machine (1)–(4) for all possible VSVs of the VSI is carried out. The second task performs the evaluation and minimization of the cost function. In general, the cost function evaluates the torque and flux error, however, several control targets, variables, and constraints can be included in a single cost function, for this reason, the cost function perform a very important role in the FS-MPC and it is possible to control several variables like flux, torque, currents, and switching frequency [30]. In this paper, the cost function is

TABLE II
POSSIBLE VSVs

δM_e	θs					
	S1	S2	S3	S4	S5	S6
$\delta M_e > 0$	U_2, U_3	U_3, U_4	U_4, U_5	U_5, U_6	U_6, U_1	U_1, U_2
$\delta M_e < 0$	U_5, U_6	U_6, U_1	U_1, U_2	U_2, U_3	U_3, U_4	U_4, U_5

defined to control the flux and torque of the machine, given by

$$F_c = \frac{1}{M_{en}} \cdot \left| M_e^* - M_e(k+2) \right| + \lambda \cdot \frac{1}{\psi_{sn}} \cdot \left| \psi_s^* - \psi_s(k+2) \right| \tag{5}$$

where M_e^* and ψ_s^* are the reference torque and reference flux, respectively; ψ_s is the magnitude of the stator flux; F_C is the value of the evaluation of each vector; M_{en} and ψ_{sn} represent the nominal torque and flux of the machine, respectively, and are used to normalize the torque and flux magnitude to obtain an equal tradeoff between the torque and flux control; and λ is the weight factor used to balance the torque and flux [31]. Finally, in order to select the optimal switching state, the cost function is evaluated for all possible VSVs of the VSI and the one that minimizes the error is selected for application in the VSI during the next control cycle.

One of the major drawbacks in FS-MPC is the evaluation of all possible VSVs of the VSI, which lead to a high computational burden and limits the sampling frequency. To overcome this problem, a simplified FS-MPC has been introduced in [19]. SFS-MPC is similar to the conventional FS-MPC and it is based on the same control structure: voltage reconstruction, estimation of the machine variables, selection of the possible VSVs, and the predictive control. The main difference compared to FS-MPC is the selection of the VSVs for prediction and actuation (see Fig. 2 red dashed line); in SFS-MPC rather to evaluate all possible VSVs, a lookup table is introduced for the selection of only three possible VSVs, and consequently, a reduction in the computational burden is obtained.

The selection of the possible VSVs is based on Table II, which evaluates the torque deviation δM_e and the angular position of the stator flux θ_s given by (6) and (7), respectively

$$\delta M_e = M_e^* - M_e \tag{6}$$

$$\theta_s = \arctan\left(\frac{\psi_\beta}{\psi_\alpha}\right). \tag{7}$$

This idea is similar to the principle of DTC, and the stationary reference frame α–β is divided into six sectors (S1–S6) every $\pi/3$ rad [see Fig. 1(b)]. Table II selects only two AVSVs and one ZVSV for evaluation in the predictive control. For instance, if the stator flux lies in the sector 1 and the torque deviation is greater than zero, the two possible AVSVs are U_2, U_3 and U_0. It can be noted from Table II that the possibility for a torque deviation equal to zero is not considered, for this reason, the ZVSV U_0 is selected to cover the case of a zero torque deviation. In this case, it is not necessary to evaluate the U_0 and U_7 vectors since both have the same effect on the machine, however, when applied

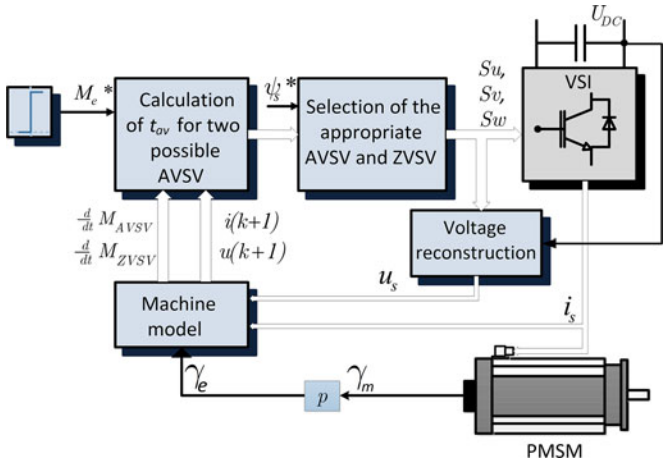

Fig. 3. Simplified block diagram of PDTC.

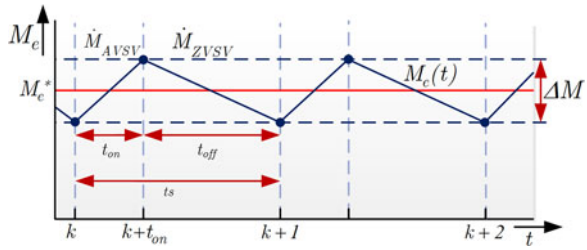

Fig. 4. Principle of the torque control in the PDTC scheme (steady state).

to the inverter, the number of switching transitions between the past VSV and the ZVSV (U_0 or U_7) are considered to reduce the switching frequency. Finally, in order to select the final vector, the three possible VSVs are predicted and evaluated using the cost function given by (5), and the one minimizing the cost function is selected for the application in the inverter during the next control cycle.

It can be noted that Table II does not take into consideration the flux variation for the preselection of the two possible AVSVs, however, this method is still valid because torque estimation is performed based on the stator current and the stator flux of the machine, moreover, the final selection is carried out based on a cost function that evaluates both the torque and flux, therefore, a satisfactory torque and flux performance is obtained.

B. PDTC and MPTC

The simplified block diagram of the PDTC is shown in Fig. 3 and it is comprised of four blocks: the voltage reconstruction, the estimation of the machine variables, the calculation of the active time for two possible AVSV and the selection of the final AVSV. In PDTC, the application of two VSVs during each control cycle is pursued, hence, unlike FS-MPC where the applied vector is kept constant during the whole control cycle, in PDTC one AVSV and one ZVSV are applied during the control cycle as shown in Fig. 4. During steady state, one AVSV is applied to the VSI for a predetermined active time t_{av}, and a ZVSV is applied during the rest of the control cycle t_{zv}. In order to keep

a fast torque response in PDTC during transients, the switching transition from an AVSV to a ZVSV is not performed and a single state is applied during the whole control cycle. By assuming a linear torque performance during the control cycle, the magnitude of the torque at $(k+1)$ can be predicted as [23]

$$M_e(k+1) = M_e(k) + \dot{M}_{\text{AVSV}} \cdot t_{av} + \dot{M}_{\text{ZVSV}} \cdot t_{zv} = M^* - \frac{1}{2}\Delta_M \tag{8}$$

where $\dot{M}_{\text{AVSV}}$ and $\dot{M}_{\text{ZVSV}}$ are the torque derivatives for the AVSV and ZVSV, respectively, and are calculated as in [22]. The principle of the PDTC is to keep the torque of the machine within the bandwidth of a virtual hysteresis Δ_M, which can be calculated from Fig. 4 as

$$\Delta_M = -\frac{\dot{M}_{\text{AVSV}} \cdot \dot{M}_{\text{ZVSV}}}{\dot{M}_{\text{AVSV}} - \dot{M}_{\text{ZVSV}}} Ts. \tag{9}$$

By solving (8) for the switching time t_{av}, the active time corresponding to a given value of torque reference can be calculated as function of the voltages, the measured currents, the permanent-magnet flux, and the rotor position; thus, the switching time t_{av} for the application of the AVSV is calculated as [22]

$$t_{av} = \frac{M^* - M_e - \frac{\Delta_M}{2} - \dot{M}_{\text{ZVSV}} \cdot Ts}{\dot{M}_{\text{AVSV}} - \dot{M}_{\text{ZVSV}}} \tag{10}$$

and the switching time t_{zv} for the application of the ZVSV as

$$t_{zv} = Ts - t_{av}. \tag{11}$$

Based on the same principle that SFS-MPC, on PDTC, two possible AVSV are selected for each control cycle and their respective active times are calculated based on (10), then, in order to select the optimal AVSV, the evaluation of the error between the reference flux and the predicted value of the flux of the machine is carried out, thus, the AVSV that yields to a minimum flux deviation from the reference is chosen for the application in the next control cycle [23].

As pointed before, in PDTC, the criterion for the final selection of the optimal AVSV is based on a second flux prediction, this is commonly seen as a drawback because of the math simplification used when the flux prediction is performed. In order to consider both the torque and flux performance for selecting the optimal AVSV, MPTC has been introduced in [27] and [28]. The simplified block diagram of the MPTC is shown in Fig. 2 (black plus blue dashed line) and it is comprised of a combined structure between the FS-MPC and the PDTC. In MPTC, the objective of the predictive control is to reduce the ripple in the controlled variables, for this reason, an AVSV is selected following the idea introduced in the FS-MPC, and subsequently, the AVSV to be applied is optimized following the procedure introduced in the PDTC.

MPTC is performed similarly to the other control techniques: first the voltage reconstruction is carried out, then, the estimation of the machine variables, and finally, the predictive control. As it can be observed in Fig. 5, the predictive control is performed into two stages: in the first stage, the selection of the AVSV that minimizes the cost function given by (5) is performed, then, the active time for the preselected AVSV is calculated using (10) and is applied to the inverter in the next control cycle.

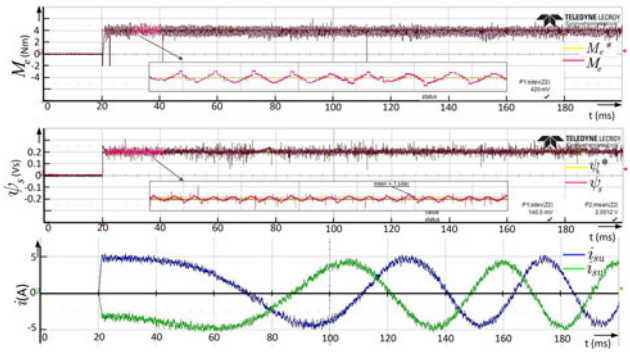

Fig. 5. FS-MPC steady state. From top: Electromagnetic torque; stator flux; stator currents.

TABLE III
PMSM PARAMETERS

Parameter	Value	Parameter	Value
Rated torque	4.7 Nm	Pole pairs	3
Stator resistance	2.41 Ω	Rated speed	3000 min^{-1}
Stator inductance	24 mH	Flux linkage PM	0.2456 Vs
Rated current	3.4 A	Rotor inertia	$3.041 \times 10^{-3}\text{kgm}^2$

IV. Comparative Evaluation

In this section, an experimental evaluation of the predictive control strategies previously described is given. The machine under test is a commercial available PMSM whose parameters are listed in Table III and is connected to a SKiiP 232GD120-313CTV, which is a two-level VSI used to feed the voltage to the machine. The angular position of the rotor is obtained from an incremental encoder of 2024 ppr, while the currents are sensed using the Hall effect sensors LTS25Np. In order to implement the controllers, an Altera Board DE2-115 with a Cyclone IV EP4CE115 device is used; all of them have been described using VHSIC[1] Hardware Description Language (VHDL) code in two complement and fixed-point arithmetic of 32 bits (1 bit for the sign, 15 bits for the real part, and 16 bits for the decimal part). The sampling time is the same for all controllers and has been set on 55 μs (18.18 kHz) in order to limit the switching frequency below the maximum frequency of the VSI (20 kHz).

The comparison is performed to evaluate the following aspects: dynamic torque response, torque and flux ripple, total harmonic distortion (THD) of the stator currents, average switching frequency, and computational effort. The selection of the value of λ is a very important issue in predictive schemes, a large value of λ would improve flux performance while torque ripple would increase, in contrast, a small value of λ would reduce torque ripple while flux performance would be deteriorated as shown in [14]. For this reason, it is important to obtain a λ value that assign a similar importance to both torque and

[1] Very high-speed integrated circuit.

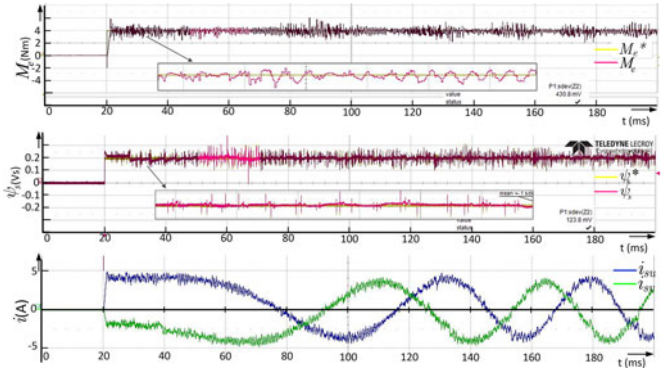

Fig. 6. SFS-MPC steady state. From top: Electromagnetic torque; stator flux; stator currents.

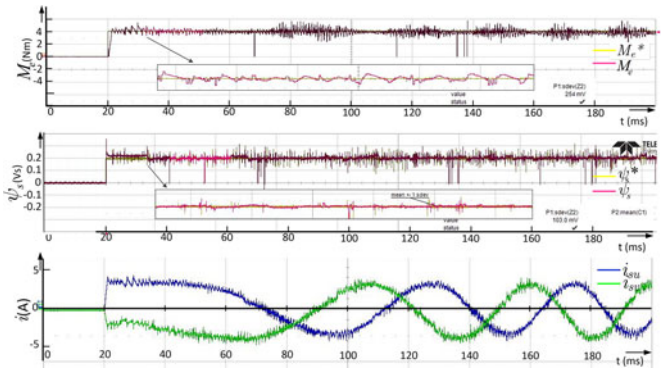

Fig. 7. PDTC steady state. From top: Electromagnetic torque; stator flux; stator currents.

stator flux. Some guidelines for the selection of the value of are presented in [31]. In the case of the FS-MPC, SFS-MPC, and MPTC, the λ factor is determined based on extensive simulation, this factor is set on 0.85 for all of them. Finally, in order to mitigate the effects of the digital delay caused by the computational burden of the predictive schemes, all of them have been compensated according to the delay-time compensation introduced in [30].

A. Experimental Results

For sake of space, results are shown for one operating point; for each predictive scheme, the torque and flux references are the same. The torque reference is set from 0 to 4 Nm; and the flux is changed using a reference from 0 to 0.2 Vs at a time of 20 ms. The performance of the predictive schemes for the PMSM are shown in Figs. 5–8; for all predictive schemes a fast dynamic response in the torque and flux is observed. It can be noted from the figures that the predictive scheme that presents the bigger torque and flux ripple is the SFS-MPC, on the other hand, the other predictive schemes present a similar performance in the flux and torque ripple. In the case of current performance, the FS-MPC presents a bigger ripple compared to the other predictive schemes.

Fig. 5 shows the experimental results of the FS-MPC. It can be noted that the torque follows the torque reference quickly. A zoom is applied to the torque and a ripple of 0.42 Nm is

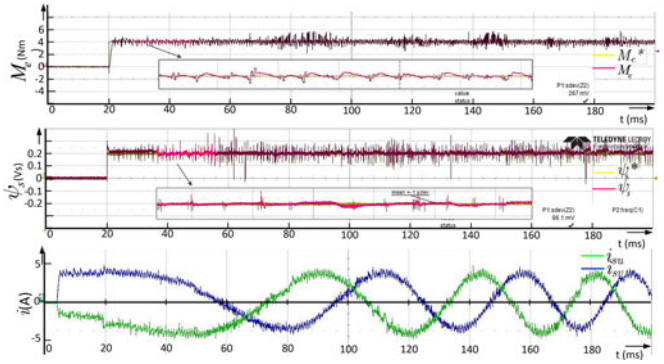

Fig. 8. MPTC steady state. From top: Electromagnetic torque; stator flux; stator currents.

calculated. The stator flux follows the flux reference immediately and a ripple of 0.014 Vs is obtained. Similar experimental results are obtained from the other predictive schemes, which successfully follow the torque and flux reference; in the case of the SFS-MPC, the ripple torque is 0.43 Nm and the flux ripple is 0.0093 Vs; in PDTC, the torque ripple is 0.254 Nm and the flux ripple is 0.0103 Vs; finally, in the MPTC, the torque ripple is 0.267 Nm and the flux ripple is 0.0086 Vs. The results obtained show an excellent torque reaction of all predictive schemes, however, a slightly difference on the ripple is observed, being the SFS-MPC and FS-MPC the ones with the largest torque, flux, and current ripple.

It can be noted from Fig. 5–8 that the predictive schemes where duty cycle is optimized outperform the predictive schemes where only one switching state is applied in the whole control cycle, nevertheless, the fact that a better performance is obtained by using a more complex implementation should be taken into account when implementing these predictive schemes for a certain application. On the other hand, it can be expected that PDTC and MPTC present a smaller torque and flux ripple than FS-MPC and SFS-MPC because of the optimization of the AVSV, however, the lack of a previous comparison has not allowed us to verify this assumption objectively, here is the importance of the presented comparison.

B. Dynamic Torque Response

The dynamic torque response is evaluated from the results showed in Fig. 5–8. The rotor is initially aligned by a pulse train to reach a zero position, for this reason, a small pulse is observed when the machine starts to operate. The zoomed torque response for each predictive scheme is shown in Fig. 9. It can be observed that a similar torque dynamic response is obtained for every predictive scheme with an approximate time of 1 ms to reach the torque reference. The reason to observe a similar behavior in the dynamic torque response is attributed to the final AVSV selected for the next control cycle, for instance, when the FS-MPC and the SFS-MPC are carried out and a dynamic change in the torque reference is observed, both controllers keep the previously selected AVSV during the whole control cycle, for this reason, their times to reach the torque reference are similar ($\approx$1 ms). On the other hand, although the PDTC and the

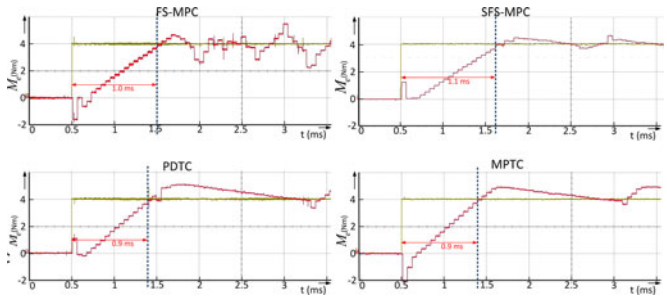

Fig. 9. Dynamic torque response.

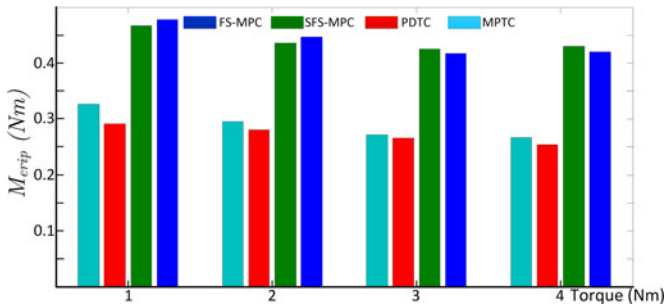

Fig. 10. Evaluation of the torque ripple under different values of torque reference.

MPTC are strategies that tend to optimize the performance by controlling the duty cycle, during dynamic response, the application of one VSV during the whole control cycle is preferred to increase the dynamic response, which is slightly faster than the FS-MPC and SFS-MPC with a time of 0.9 ms.

C. Torque and Flux Ripple

The evaluation of the torque and flux ripple is carried out by using the standard deviation of the torque M_{erip} and flux ψ_{srip} given by (12) and (13), and is expressed in terms of percentage performance through the coefficient of variation of torque $\%M_{\text{erip}}$ and flux $\%\psi_{\text{srip}}$ as (14)

$$M_{\text{erip}} = \sqrt{\frac{1}{N}\sum_{i=1}^{N}\left(M_e(i) - {M_e}^*\right)^2} \tag{12}$$

$$\psi_{\text{srip}} = \sqrt{\frac{1}{N}\sum_{i=1}^{N}\left(\psi_s(i) - {\psi_s}^*\right)^2} \tag{13}$$

$$\%M_{\text{erip}} = \frac{M_{\text{erip}}}{M_e^*} \cdot 100 \tag{14a}$$

$$\%\psi_{\text{srip}} = \frac{\psi_{\text{srip}}}{\psi_s^*} \cdot 100. \tag{14b}$$

The torque ripple evaluation of each predictive scheme at different torque references is shown in Fig. 10. It can be observed that the control algorithm that presents the lowest torque ripple is the PDTC; and that the SFS-MPC is the control algorithm that presents the biggest ripple of all presented schemes. A better performance is obtained when the PMSM is operating close the nominal torque, thus, when the machine operates at a 4-Nm torque reference, the FS-MPC present a ripple

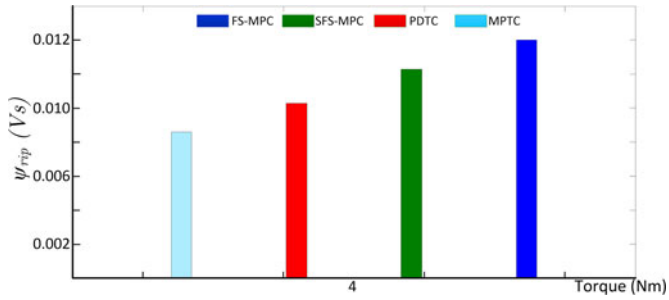

Fig. 11. Evaluation of the flux ripple under different a 4-Nm torque reference.

of 0.42 Nm (10.5%), while a ripple of 0.43 Nm (10.75%), 0.254 Nm (6.35%), and 0.267 Nm (6.67%) are obtained for the SFS-MPC, PDTC, and MPTC, respectively. On the other hand, the torque ripple presents a slight increment when the PMSM is operating at lower torque references; this variation on the ripple performance is congruent with the efficiency of an electric drive, which is better when the machine operates close to the nominal values [32]. One aspect to highlight of the torque ripple evaluation is that an optimization procedure in the application of the optimal AVSV directly affects the ripple in the torque of the machine; consequently, when the duty-cycle optimization is carried out, a better torque and flux performance is obtained. Conversely, when constraints are introduced to determine the possible AVSV for the next control cycle (see Table II) in SFS-MPC, a slight increment in the torque ripple is obtained; this is caused because the optimal VSV may not be preselected using Table II.

The results of the flux ripple evaluation under a torque reference of 4 Nm is shown in Fig. 11. The experimental results show that the variation of the flux ripple under different torque references is smaller compared to the variation on the torque ripple of the PMSM, for this reason, the evaluation of the flux ripple is only presented for the case of the 4-Nm torque reference. Here, the FS-MPC is the predictive scheme that presents the highest ripple with a 0.014 Vs (7%) of flux ripple; however, the predictive scheme that presents the lowest ripple is the MPTC with a flux ripple of 0.0086 Vs (4.3%). The remaining predictive schemes presents a flux ripple of 0.0123 Vs (6.15%) and 0.0103 Vs (5.15%) for the SFS-MPC and the PDTC, respectively.

D. Stator Current THD

The THD is calculated by

$$\text{THD} = \frac{\sqrt{I_2^2 + I_3^2 + \cdots + I_n^2}}{I_F} \tag{15}$$

where I_n is the RMS value of the harmonic n, and I_F is the RMS value of the fundamental current. Fig. 12 shows the evaluation of THD for each predictive scheme when a reference of 4 Nm is applied to the machine. The predictive scheme that presents the bigger THD is the FS-MPC with a 12.54%. A remarkable difference is observed with the other predictive schemes where a THD of 12.42%, 9.51%, and 9.57% is obtained for the SFS-MPC, PDTC, and MPTC, respectively. It can be observed from Fig. 12 that the PDTC is the predictive scheme with the lower harmonics components followed by the MPTC, conversely, the

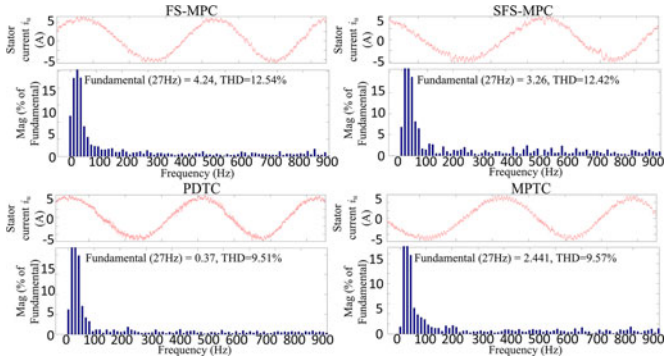

Fig. 12. Stator current THD.

FS-MPC and the SFS-MPC presents a more spread harmonic spectrum.

E. Average Switching Frequency

In order to evaluate the average switching frequency f_{sw} of each predictive scheme, the following expression is used [6]:

$$f_{\text{sw}} = \frac{1}{3}\frac{Na + Nb + Nc}{T} \tag{16}$$

where Na, Nb, and Nc are the number of switching cycles in one switch of the phases a, b, and c, respectively; and T is the period considered for the calculation of the f_{sw}.

The f_{sw} of each predictive scheme under different speed and torque references is shown in Fig. 13. The SFS-MPC is the predictive scheme that presents the lowest f_{sw} below 3 kHz, and is followed by the FS-MPC with an average of 3 kHz; conversely, the PDTC is the predictive scheme that presents the biggest f_{sw} of approximately 8 kHz; and finally, the MPTC presents a f_{sw}, which vary from 5 to 7 kHz. A significant difference in the f_{sw} between the predictive schemes with duty-cycle control (PDTC and MPTC) and the other schemes (FS-MPC and SFS-MPC) can be observed, this issue is related to the duty cycle that causes the power semiconductors to maintain a fixed switching frequency during steady state in PDTC and MPTC, however, in FS-MPC and SFS-MPC, the switching frequency is always variable.

F. Computational Effort

The computational effort of each predictive algorithm is evaluated based on the execution time and the number of resources used for its implementation, and is performed for an Altera Board DE2-115 with a Cyclone IV EP4CE115 with an internal clock of 50 MHz. The execution time of each predictive scheme is summarized in Table IV. Each predictive scheme presents a quite similar execution time, here is observed that PDTC is the fastest algorithm, while the FS-MPC is the slowest. A significant time execution is observed during the signal conditioning, this time is caused by the analog-to-digital conversion (ADC) and digital-to-analog conversion (DAC), which can be significantly reduced by using a much faster ADC and DAC converter.

Table V shows the summary of used resources for each predictive scheme. PDTC is the control scheme that needs

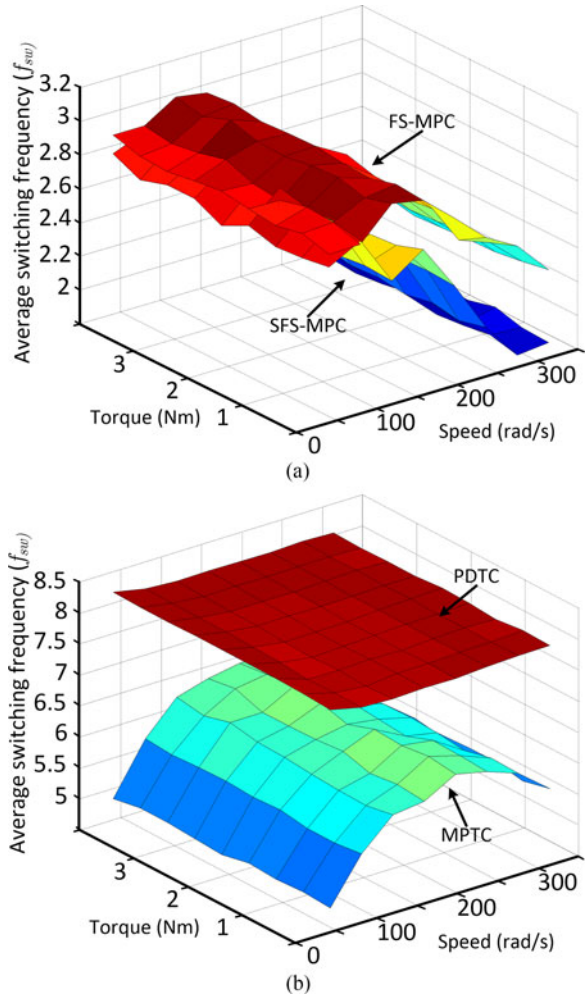

Fig. 13. Average switching frequency under different speed and torque references. (a) FS-MPC and SFS-MPC. (b) PDTC and MPTC.

TABLE IV
EXECUTION TIME

	Control Algorithm	*Signal Conditioning*	*Total Execution Time*
FS-MPC	12.52 μs	31.94 μs	44.46 μs
SFS-MPC	11.16 μs	31.94 μs	43.1 μs
PDTC	9.76 μs	31.94 μs	41.7 μs
MPTC	11.48 μs	31.9 μs	43.38 μs

TABLE V
SUMMARY OF USED RESOURCES

	Total Logic Elements	*Embedded Multiplier 9-bit Elements*	*Maximum Operating Frequency*
FS-MPC	11 962/114 480 (10%)	206/532 (39%)	85.98 MHz
SFS-MPC	16 546/114 480 (14%)	318/532 (60%)	81.77 MHz
PDTC	22 218/114 480 (19%)	478/532 (90%)	62.54 MHz
MPTC	19 575/114 480 (17%)	444/532 (83%)	62.34 MHz

more resources for its implementation. In contrast, the control scheme that uses the least amount of resources is the FS-MPC. The maximum operating frequency is also showed in Table V. Here, the MPTC presents the lowest maximum operating frequency, while the FS-MPC presents the biggest operating frequency. Results from Tables IV and V may vary depending on the digital platform, however, is the intention of the authors to give a parameter for the evaluation of the complexity of each predictive scheme to point out the main differences in execution time and used resources.

The timing performance and the number of used resources vary depending on the control algorithm as observed in Tables IV and V. One important aspect to highlight is that the number of used resources varies in each predictive scheme according to the complexity, while in PDTC and MPTC, a high amount of resources are used; this is not the case of FS-MPC and SFS MPC. In the same way, the number of used resources in the predictive schemes that only evaluate three VSVs (SFS-MPC and PDTC) are not necessary lower than those who perform the full evaluation of each VSV of the VSI (FS-MPC and PDTC). The reason for this is because in SFS-MPC and PDTC, the angular position of stator flux, torque deviation, and the selection of the possible VSVs, based on Table II, are integrated into the control scheme, thus, a slight increment in the number of used resources is obtained. From these results, it can be concluded that a tradeoff between the performance and the number of resources needed for implementation is presented, here, in order to obtain a better torque and flux performance, a more complex algorithm is needed, thus, a more number of digital resources are needed.

V. Discussion and Conclusion

In this paper, the comparison of four predictive schemes for a PMSM has been presented. The comparison is performed to evaluate different characteristics: the torque performance in steady and dynamic state, torque and flux ripple, current THD, average switching frequency, and computational effort.

Experimental results have shown that the predictive scheme that presents the poorest performance is the SFS-MPC, with largest torque and flux ripple, as well as a larger THD and a more spread harmonic spectrum, which is something not desirable in certain applications. SFS-MPC is followed by the FS-MPC in terms of performance. On the other hand, the more reduced torque and flux ripple is obtained with the PDTC, however, the digital resources for its implementation is higher than the FS-MPC and SFS-MPC. In the case of dynamic behavior, all algorithms present a similar rising time because the VSV applied during transients is quite similar, here, in all predictive schemes, only one switching state is applied during dynamics. In terms of the current THD, the PDTC is the predictive scheme that presents the lowest spread harmonic spectrum. The average switching frequency is quite different in each predictive scheme, FS-MPC and SFS-MPC presents the lowest switching frequency, while the PDTC presents the biggest switching frequency. Finally, the algorithm complexity was evaluated, although the execution time of each predictive scheme is comparable, a higher amount of resources is needed for the PDTC and MPTC.

In terms of performance, it can be noted that all predictive schemes present an excellent flux and torque performance. It has been showed that duty-cycle optimization yields to a lower flux and torque ripple in expense of a more complex control where more digital resources are needed. Conversely, in FS-MPC and SFS-MPC, the performance is still notable; however, a larger ripple is obtained. For a final choice of the control algorithm, it is important to consider objectives and constraints, for instance, for an application where torque ripple is not a very important issue the use of a simpler controller (FS-MPC and SFS-MPC) that still performs remarkable and the use of a lower cost digital platform can be afforded, however, if lower torque ripples are necessary, a most complex control scheme (PDTC and MPTC) will be necessary, as well as a more powerful digital platform.

The experimental results presented in this paper confirm that predictive schemes are a competitive alternative to classical vector control schemes, however, this results also intend to serve as a starting point for researchers that are interested in the field of predictive control for future selection of predictive schemes, since there are different predictive schemes, it is not a trivial task to select the one that fit better their control objectives, and so far, there is not a comparison of the most used predictive schemes presented in the literature.

Acknowledgment

The authors would like to thank the Altera University Program for the donation of Altera board DE2-115 used to carry out this investigation.

References

[1] W. U. Bin, *High Power Converters and AC Drives*. Piscataway, NJ, USA: IEEE Press, 2006.

[2] P. Cortes, M. P. Kazmierkowski, R. M. Kennel, D. E. Quevedo, and J. Rodriguez, "Predictive control in power electronics and drives," *IEEE Trans. Ind. Electron.*, vol. 55, no. 12, pp. 4312–4324, Dec. 2008.

[3] J. Rodriguez *et al.*, "State of the art of finite control set model predictive control in power electronics," *IEEE Trans. Ind. Informat.*, vol. 9, no. 2, pp. 1003–1016, May 2013.

[4] K. Belda and D. Vošmik, "Explicit generalized predictive control of speed and position of PMSM drives," *IEEE Trans. Ind. Electron.*, vol. 63, no. 6, pp. 3889–3896, Jun. 2016.

[5] P. Alkorta, O. Barambones, J. A. Cortajarena, and A. Zubizarrreta, "Efficient multivariable generalized predictive control for sensorless induction motor drives," *IEEE Trans. Ind. Electron.*, vol. 61, no. 9, pp. 5126–5134, Sep. 2014.

[6] H. A. Young, M. A. Perez, J. Rodriguez, and H. Abu-Rub, "Assessing finite-control-set model predictive control: A comparison with a linear current controller in two-level voltage source inverters," *IEEE Ind. Electron. Mag.*, vol. 8, no. 1, pp. 44–52, Mar. 2014.

[7] S. Vazquez *et al.*, "Model predictive control: A review of its applications in power electronics," *IEEE Ind. Electron. Mag.*, vol. 8, no. 1, pp. 16–31, Mar. 2014.

[8] J. Rodriguez, P. Cortes, R. Kennel, and M. P. Kazrnierkowski, "Model predictive control—A simple and powerful method to control power converters," in *Proc. IEEE 6th Int. Power Electron. Motion Control Conf.*, Wuhan, China, 2009, pp. 41–49.

[9] S. Kouro, M. A. Perez, J. Rodriguez, A. M. Llor, and H. A. Young, "Model predictive control: MPC's role in the evolution of power electronics," *IEEE Ind. Electron. Mag.*, vol. 9, no. 4, pp. 8–21, Dec. 2015.

[10] J. Scoltock, T. Geyer, and U. K. Madawala, "A comparison of model predictive control schemes for MV induction motor drives," *IEEE Trans. Ind. Inf.*, vol. 9, no. 2, pp. 909–919, May 2013.

[11] T. Geyer, "A comparison of control and modulation schemes for medium-voltage drives: Emerging predictive control concepts versus PWM-based schemes," *IEEE Trans. Ind. Appl.*, vol. 47, no. 3, pp. 1380–1389, May/Jun. 2011.
[12] F. Wang, S. Li, X. Mei, W. Xie, J. Rodríguez, and R. M. Kennel, "Model-based predictive direct control strategies for electrical drives: An experimental evaluation of PTC and PCC methods," *IEEE Trans. Ind. Informat.*, vol. 11, no. 3, pp. 671–681, Jun. 2015.
[13] F. Niu, B. Wang, A. S. Babel, K. Li, and E. G. Strangas, "Comparative evaluation of direct torque control strategies for permanent magnet synchronous machines," *IEEE Trans. Power Electron.*, vol. 31, no. 2, pp. 1408–1424, Feb. 2016.
[14] Y. Zhang, H. Yang, and B. Xia, "Model-predictive control of induction motor drives: Torque control versus flux control," *IEEE Trans. Ind. Appl.*, vol. 52, no. 5, pp. 4050–4060, Sep./Oct. 2016.
[15] H. Miranda, P. Cortes, J. I. Yuz, and J. Rodriguez, "Predictive torque control of induction machines based on state-space models," *IEEE Trans. Ind. Electron.*, vol. 56, no. 6, pp. 1916–1924, Jun. 2009.
[16] E. Fuentes, D. Kalise, J. Rodríguez, and R. M. Kennel, "Cascade-free predictive speed control for electrical drives," *IEEE Trans. Ind. Electron.*, vol. 61, no. 5, pp. 2176–2184, May 2014.
[17] M. Preindl and S. Bolognani, "Model predictive direct speed control with finite control set of PMSM drive systems," *IEEE Trans. Power Electron.*, vol. 28, no. 2, pp. 1007–1015, Feb. 2013.
[18] T. Geyer and D. E. Quevedo, "Multistep finite control set model predictive control for power electronics," *IEEE Trans. Power Electron.*, vol. 29, no. 12, pp. 6836–6846, Dec. 2014.
[19] M. Habibullah, D. D. C. Lu, D. Xiao, and M. F. Rahman, "A simplified finite-state predictive direct torque control for induction motor drive," *IEEE Trans. Ind. Electron.*, vol. 63, no. 6, pp. 3964–3975, Jun. 2016.
[20] C. Xia, T. Liu, T. Shi, and Z. Song, "A simplified finite-control-set model-predictive control for power converters," *IEEE Trans. Ind. Informat.*, vol. 10, no. 2, pp. 991–1002, May 2014.
[21] I. Alevras, P. Karamanakos, S. Manias, and R. Kennel, "Variable switching point predictive torque control with extended prediction horizon," in *Proc. 2015 IEEE Int. Conf. Ind. Technol.*, Seville, Spain, 2015, pp. 2352–2357.
[22] M. Pacas and J. Weber, "Predictive direct torque control for the PM synchronous machine," *IEEE Trans. Ind. Electron.*, vol. 52, no. 5, pp. 1350–1356, Oct. 2005.
[23] R. Morales-Caporal, E. Bonilla-Huerta, M. A. Arjona, and C. Hernández, "Sensorless predictive DTC of a surface-mounted permanent-magnet synchronous machine based on its magnetic anisotropy," *IEEE Trans. Ind. Electron.*, vol. 60, no. 8, pp. 3016–3024, Aug. 2013.
[24] P. Karamanakos, P. Stolze, R. M. Kennel, S. Manias, and H. du Toit Mouton, "Variable switching point predictive torque control of induction machines," *IEEE J. Emerg. Sel. Topics Power Electron.*, vol. 2, no. 2, pp. 285–295, Jun. 2014.
[25] Y. Zhang and J. Zhu, "Direct torque control of permanent magnet synchronous motor with reduced torque ripple and commutation frequency," *IEEE Trans. Power Electron.*, vol. 26, no. 1, pp. 235–248, Jan. 2011.
[26] Y. Zhang and J. Zhu, "A novel duty cycle control strategy to reduce both torque and flux ripples for DTC of permanent magnet synchronous motor drives with switching frequency reduction," *IEEE Trans. Power Electron.*, vol. 26, no. 10, pp. 3055–3067, Oct. 2011.
[27] Y. Zhang, H. Yang, and B. Xia, "Model predictive torque control of induction motor drives with reduced torque ripple," *IET Elect. Power Appl.*, vol. 9, no. 9, pp. 595–604, Nov. 2015.
[28] Y. Zhang and H. Yang, "Model predictive torque control of induction motor drives with optimal duty cycle control," *IEEE Trans. Power Electron.*, vol. 29, no. 12, pp. 6593–6603, Dec. 2014.
[29] S. A. Davari, D. A. Khaburi, and R. Kennel, "An improved FCS–MPC algorithm for an induction motor with an imposed optimized weighting factor," *IEEE Trans. Power Electron.*, vol. 27, no. 3, pp. 1540–1551, Mar. 2012.
[30] P. Cortes, J. Rodriguez, C. Silva, and A. Flores, "Delay compensation in model predictive current control of a three-phase inverter," *IEEE Trans. Ind. Electron.*, vol. 59, no. 2, pp. 1323–1325, Feb. 2012.
[31] P. Cortes *et al.*, "Guidelines for weighting factors design in model predictive control of power converters and drives," in *Proc. IEEE Int. Conf. Ind. Technol.*, Feb. 10–13, 2009, pp. 1–7.
[32] P. Waide and C. U. Brunner, "Energy-efficiency policy opportunities for electric motor-driven systems," International Energy Agency, Paris, France, 2011.

Omar Sandre-Hernandez received the B.Sc. degree in mechatronics engineering from the University of the Mexican Valley, Mexico City, Mexico, in 2010, and the Master's degree in computer systems from the Postgraduate Studies and Research Division, Technological Institute of Apizaco, Apizaco, Mexico, in 2012. He is currently working toward the Ph.D. degree in electronics engineering with the National Institute for Astrophysics, Optics, and Electronics, Puebla, Mexico.

His research interests include power electronics, motor control, sensorless control, and digital control.

Jose Rangel-Magdaleno (S'08–M'13–SM'17) received the B.E. degree in electronics engineering and the M.E. degree in electrical engineering on hardware signal processing from the Universidad de Guanajuato, Guanajuato, Mexico, in 2006 and 2008, respectively, and the Ph.D. degree from the Universidad Autonoma de Queretaro, Santiago de Querétaro, Mexico, in 2011.

He is currently a Full Researcher with the Electronics Department, National Institute for Astrophysics, Optics, and Electronics, Puebla, Mexico. He has authored one book and more than 65 works published in book chapters, journals and conferences. His research interests include FPGAs, signal and image processing, instrumentation, and mechatronics.

Dr. Rangel-Magdaleno is a Member of the Mexican National Research System (SNI), Level 1.

Roberto Morales-Caporal (S'05–M'08–SM'14) received the B.Sc. degree in electromechanical engineering from the Technological Institute of Apizaco, Apizaco, Mexico, in 1999, the M.Sc. degree in electrical engineering from the Graduate and Research Department, Superior School of Mechanical and Electrical Engineering, National Polytechnic Institute (IPN), Mexico City, Mexico, in 2001, and the Dr.-Ing. degree in electrical engineering from the University of Siegen, Siegen, Germany, in 2007.

From 2001 to 2003, he was a Lecturer with the Interdisciplinary Professional Unit on Engineering and Advanced Technologies, IPN. Since 2008, he has been with the Postgraduate Studies and Research Division, Technological Institute of Apizaco. His research interests include motor control, sensorless control, control of power converters for renewable energy, and digital-signal-processor-based digital control.

Dr. Morales-Caporal was the recipient of the First Prize Paper Award from the Technical Committee on Electrical Machines of the IEEE Industrial Electronics Society in 2009. He was also the recipient of a scholarship awarded by the German Academic Exchange Service for doctoral studies in 2003. He is a member of the Mexican National Research System (SNI), Level 1.